Advanced Ranging Instrumentation

Meegyeong Paik,* James S. Border,† Stephan Esterhuizen,‡ and Dong K. Shin†

ABSTRACT. — Ranging measurements in the Deep Space Network (DSN) have been contributing to spacecraft navigation and radio science investigations for more than a half century. Performance over the past three decades has remained at the 1-m level conditionally due to solar plasma noises and has also been limited by systematic instrumental effects. Since the goal of 10-cm ranging has long been sought, JPL has invested in the design and development of an Advanced Ranging Instrument (ARI) that will improve the accuracy of ranging measurements by one order of magnitude. The current ranging uses a single-frequency uplink, 7.1 GHz (X-band). By using dual-frequency uplinks, X and 34 GHz (Ka-band), and generating three downlinks (X-up/X-down, X-up/Ka-down, Ka-up/Ka-down), the noise of solar plasma can be removed completely. Also, station delay is measured continuously to obtain a precise calibration. Implementing wideband pseudo-random noise (PN) code ranging further reduces system noises. The ARI has made these techniques available at DSS-25. This new ranging will enhance planetary sciences and fundamental physics as well as orbit determination and navigation.

I. Introduction

Precise microwave tracking of interplanetary spacecraft has been a crucial tool in solar system exploration. Experience with the multi-frequency radio links with Cassini has demonstrated orders of magnitude improvement in precision Doppler for radio science measurements, which include some of the most stringent limits on deviations from Einstein's Theory of General Relativity (GR). The upcoming ESA BepiColombo mission to Mercury presents an important opportunity to improve on these radiometric limits, but only if the Deep Space Network (DSN) is equipped with advanced ranging science instrumentation. This report describes an ongoing Research and Technology Development (R&TD) task, along with supporting DSN upgrades, to develop and deploy this science augmentation, and thereby provide JPL scientists with the opportunity to maintain and enhance their leadership position in radio science measurements.

Range and range rate measurements, the main radiometric observable quantities in spacecraft orbit determination and navigation, have been widely used to refine the

---

dynamical model of the solar system and to probe planetary interiors. The radio science experiments of the Cassini mission to Saturn have demonstrated a significant improvement in microwave tracking systems using multi-frequency radio links that include 32 GHz (Ka-band). At very small Sun-Earth-Probe (SEP) angles, nearly complete calibration of the propagation noise from the interplanetary plasma using the multi-frequency links, and highly accurate calibration of the neutral troposphere using an advanced water vapor radiometer, resulted in range-rate accuracy as small as 2 μm/s (one way at 300 s averaging), a factor of 600 better than the corresponding un-calibrated ones [1]. As a result of this advancement, the Cassini radio system has greatly contributed to making the most accurate test of GR with spacecraft Doppler to date—for instance, the Cassini limit on post-Newtonian parameter $\gamma = 1 + (2.1 \pm 2.3) \times 10^{-5}$ [2].

Cassini measured the range-rate but not range because the latter was not an available spacecraft capability or ground station capability at Ka-band. Ranging was available at 8.4 GHz (X-band), and the plasma error contribution limited its accuracy to the 1-m level in one-way range.

However, systems are evolving. While Cassini had Doppler at X- and Ka-bands and ranging only at X-band, the next mission of interest will have both Doppler and ranging at X- and Ka-bands. The ESA BepiColombo mission to Mercury has implemented further developments in the radio instrumentation, Mercury Orbit Radio Experiment (MORE), to achieve a one-way range accuracy of 10 cm (at integration times of a few seconds) by enabling multi-frequency links and a higher precision ranging code. The stringent requirements for BepiColombo's ranging function can be met only by considering a complete plasma calibration on the ranging observable. This implies that the ranging turnaround function must be implemented on all three frequency links (X up/X down, X up/Ka down, and Ka up/Ka down). The key instrument is a Ka/Ka band digital transponder on the spacecraft that enables a high phase coherence between uplink and downlink carriers and supports a wideband ranging code that is required to obtain high ranging accuracy for comparable integration times. The MORE radio instrument was provided to the BepiColombo mission by the Italian Space Agency.

In order to obtain the desired ranging precision, the onboard instrumentation must be complemented by a ground system based on the simultaneous transmission and reception of multiple frequencies at X- and Ka-band. DSS-25, a 34-m antenna at Goldstone, California, is one of very few facilities worldwide capable of operating at Ka-band uplink and downlink. The U.S. members of the MORE team proposed the utilization of this asset for the BepiColombo radio science investigations and further proposed the development of a specialized Ka-band ranging system.

The primary goal of this development is to build Advanced Ranging Instrumentation (ARI) that supports a wideband ranging code, and simultaneously transmits and receives multiple frequencies at X- and Ka-band. The pseudo-random noise (PN) codes recommended by the Consultative Committee for Space Data Systems (CCSDS) are implemented [3]. This high-precision ranging system on DSS-25 is able to calibrate plasma delay through the multi-frequency links and also station delay through continuous measurement. As a result, it is expected that the ranging system is capable of producing

range measurements with a one-way range accuracy of 10 cm using integration times of a few seconds, independent of the SEP angles.

II. Enhancements of Science and Technology

GR has passed many experimental tests, the latest of which was obtained in 2003 by Doppler tracking of the Cassini spacecraft [2]. However, it is unlikely that GR is the ultimate theory of gravity, and the intrinsic incompatibility of GR with quantum mechanics has motivated a long and still unsuccessful search for violations of Einstein's paradigm. For testing violations of GR, much more highly accurate determination of the post-Newtonian parameters (about a level of 10^{-7}) is required, and there is no better solar system body than Mercury on which to carry out such tests.

Located deep in the solar gravitational field and moving with a high velocity, Mercury is more affected by relativistic effects than any other solar system body. The proximity to the Sun, with frequent solar conjunctions, allows for repeated classical tests of GR with improved accuracy, as well as new experiments based on different observable quantities. The improved ranging performance will produce a 10× improvement in the constraint on the post-Newtonian parameter gamma (post-Newtonian parameters represent how GR differs from Newtonian gravity, and gamma describes the gravitational deflection of light by visible matter). Moreover, improved ranging will allow an improved determination of the orbit of Mercury, which in turn will provide a 20× improvement in the determination of the solar oblateness, a direct and unequivocal measurement of the Sun's J2, and a better upper limit (or a detection) of a possible secular change of its gravitational parameter (GM) due to a cosmological variation of gravitational constant G. The radio science experiments will be able to test the equivalent principle in its very strong form with unprecedented accuracy. All these scientific goals are of great importance to cosmology, gravitation, and solar physics.

The physical quantities of interest will be determined with an accuracy ultimately related to the performance of the range and range-rate systems. The scientific objectives in planetary geophysics and fundamental physics require the same instrumentation and data analysis procedure. Indeed, the observable quantities are the same for both classes of experiments, and the determination of all physical parameters is usually attained by means of a single, global orbital solution. Most of the present knowledge on the planetary gravity fields and interiors has been derived from accurate spacecraft tracking and precise orbit determination. Interplanetary tracking systems rely on microwave links for obtaining the key navigational data, namely the propagation time and frequency of radio signals (range and range-rate). These observable quantities are inputs to complex orbit determination codes, where the observed quantities are compared with their predicted values to produce an estimate of the spacecraft state and other parameters of the model. In planetary geodesy, the estimated quantities are typically the coefficients of the spherical harmonics expansion of a gravity field.

While the primary motivation for this development is the fundamental physics and planetary science enabled by the implementation of an advanced ranging capability for DSS-25, the advanced ranging may also prove beneficial for future, high-precision

interplanetary navigation. This system may also be beneficial as a unique ground station with advanced ranging capability.

Advanced ranging can enable future planetary missions to conduct precision exploration of their environments, especially at Mercury, where the solar plasma will otherwise dominate the noise in the tracking data. This new ranging system can expedite more precise global orbit solutions with higher ranging accuracy and promote future missions that have the capability of coherent communications and ranging modulation at X-band and Ka-band simultaneously.

The ARI technology demonstration at DSS-25 could encourage other missions to request advanced ranging and lead to a development effort to add advanced ranging as a future DSN standard service. Using CCSDS ranging codes would be another step toward standardization of tracking service support between the space agencies.

III. Observable Definition and Error Budget

The current DSN operational ranging system operates with an X-band uplink. Uplink can be either a sequence of sinusoids at several prescribed frequencies or a PN code. Either type of signal can be transponded in a transparent way by the spacecraft. The New Horizons spacecraft can also lock to a PN uplink and regenerate the PN ranging code onboard to provide much improved link performance. It is expected that future generations of transponders will routinely provide regenerative PN ranging capability.

The current DSN operational ranging system is described by Berner [4]. The ranging code phase is measured in real time using closed-loop techniques. The system is primarily operated at X-band uplink and X-band downlink. The primary ranging uplink is a 1 MHz sine wave. This primary code frequency is referred to as the ranging clock. The error budget has been developed from analysis of all phenomena affecting the signal transmission from ground station transmitter to spacecraft to ground station receiver. The error budget for the X/X link is well understood [5, 6], and has been validated by decades of spacecraft ranging data.

Ranging measurements using open-loop techniques have also been demonstrated by the DSN [7].

Figure 1 shows a block diagram of the key station ranging system components. The uplink signal is generated by the exciter, and the range code phase ϕ_{UL} is measured at the point of origin. A coupler sends a copy of the radio frequency (RF) uplink signal to a device known as the test translator that translates the frequency of the signal from the uplink band to the downlink band. This signal is then received through the normal station downlink path by both the open-loop receiver (OLR) and by the closed-loop receiver in the downlink tracking and telemetry (DTT) subsystem. Data from the DTT subsystem are available in real time, but OLR data require post-processing.

It is intended to tune the test translator so that the downlink frequency of the test signal is close to that of the received spacecraft signal. There will need to be some frequency

separation to avoid interference, but the intent is to calibrate the downlink signal path near the spacecraft frequency.
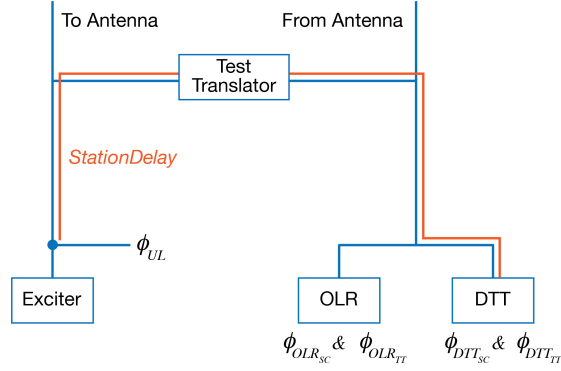

Figure 1. Simplified block diagram of station ranging system components.

Both the ranging signal received from the spacecraft (SC) and the ranging signal received from the translated test signal (TT) can be measured by either the OLR or the DTT subsystem. The measurement is of the phase of the range code. The path in Figure 1 shown in orange is known as the "station delay" calibration for the DTT. The purpose is to remove the path delay through station components that are not common to the signal propagation path between the antenna reference location and the spacecraft. Currently, station delay is normally measured at a time t_0 prior to the start of the spacecraft ranging. Using units of range code phase, station delay is defined by

$$Station\ Delay = \phi_{UL}\left(t_0\right) - \phi_{DTT_{TT}}\left(t_0\right). \tag{1}$$

The closed-loop ranging observable is defined by

$$R_{CL}\left(t\right) = \phi_{UL}\left(t\right) - \phi_{DTT_{SC}}\left(t\right) - Station\ Delay \tag{2}$$

The open-loop ranging observable is defined by

$$R_{OL}\left(t\right) = \phi_{OLR_{TT}}\left(t\right) - \phi_{OLR_{SC}}\left(t\right) \tag{3}$$

Station delay is nearly constant, but it may vary at the nanosecond level over a pass. The open-loop technique allows for continual measurement of station delay. It should be noted that if station delay were measured by the DTT subsystem at the measurement time t instead of at the earlier time t_0, then the formulations for open-loop and closed-loop range would be identical. It could also be noted that the open-loop system could measure station delay once at the beginning of a pass and then use the same formulation as for closed-loop ranging.

Either open-loop or closed-loop techniques could be used to acquire ranging data for radio science purposes. Besides providing improved measurements of station delay, open-loop techniques have the advantage that more signal-processing options are available to extract code phase for perturbed signals near solar conjunction periods.

Figure 2 shows the ranging error budget for the current DSN X/X system and also for the new ARI. The solar plasma noise at 30 degree of SEP angle is shown in the graph. Several factors have come together to provide the improvements from the X/X system to the advanced system. The charged particle errors due to solar plasma and Earth ionosphere, which have an f^{-2} frequency dependence, are nearly eliminated by a linear combination of the three received frequency links. The higher frequency ranging clock and continuous measurement of the test signal through the station electronics improve the station delay calibration. Thermal noise is greatly reduced by the higher frequency ranging clock and by the spacecraft regeneration of the PN code. The performance indicated for the spacecraft transponder assumes an improved design, as has been implemented for BepiColombo. In units of one-way distance, the ranging performance for ARI is expected to be in the order of 10 cm.
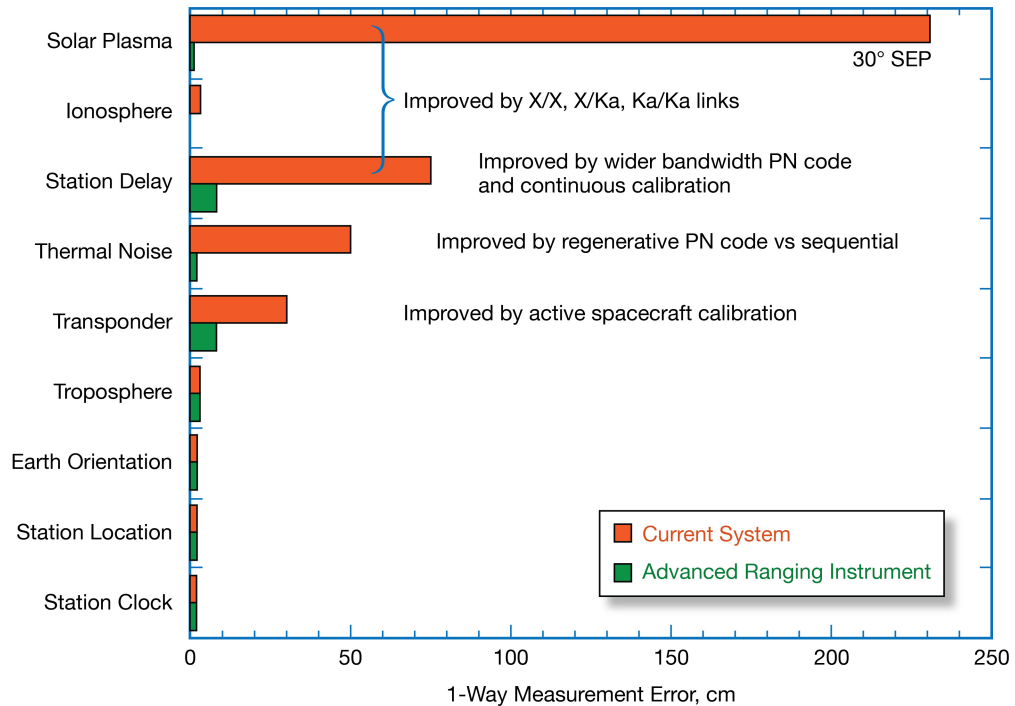

Figure 2. Ranging error budgets for current X/X system and for the ARI. Key factors that improve performance are identified.

IV. Ka-band Uplink and Range Corrections

In addition to standard X-up/X-down ranging, the DSN has long been capable of ranging with an X-up/Ka-down link. This was demonstrated during the MRO cruise from Earth to Mars [8]. However, prior to the completion of the ARI task work, the DSN had no capability for ranging on a link with Ka-band uplink. To add this capability the, following was done as part of the ARI task:

- The uplink control software was modified to enable ranging on a Ka-band uplink.

- The uplink signal generator was modified to provide a PN ranging signal using either the CCSDS T2B or T4B code and with a chip rate up to 24 Mchip/s.

- The block VI exciter was modified to provide modulation on a Ka-band uplink signal.

- A zero delay device (ZDD) for the Ka/Ka links was built to calibrate the test translator for this link.

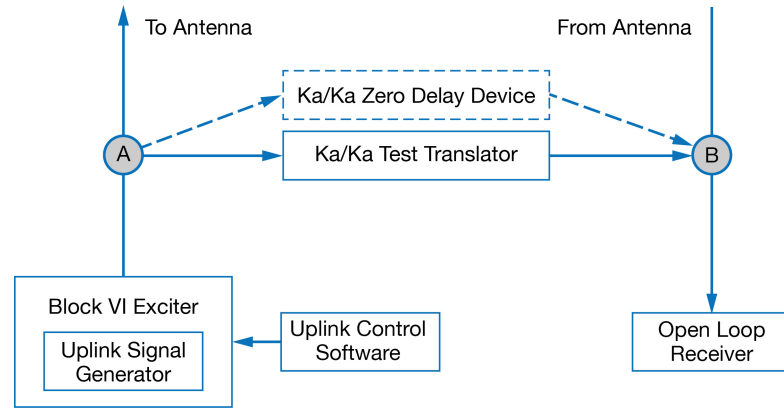- Scripts were developed for recording high chip rate ranging data on the OLR.

Figure 3. Ranging system components for the Ka/Ka link

V. Ka-band Uplink and Range Corrections

The DSN ranging measurement includes the station instrumental path delay that needs to be compensated, referring them to the Deep Space Station (DSS) reference location where the primary and secondary axis intersects. The DSN performs two independent measurements to determine the instrumental path delay: station delay calibration and z-height correction (ZCR). The station delay calibration is the delay from the uplink subsystem where the uplink ranging code is generated, to the test translator, and then to the downlink subsystem where the ranging code is received/processed. Figure 3 shows the station delay calibration path, from the uplink subsystem to A to B to the downlink subsystem. The test translator converts the uplink frequency to the downlink frequency. The ZCR is a correction offset that accounts for delays in the signal path not included in the station delay calibration measurement, namely (i) the delay of the test translator (A to B) minus (ii) the delay between A and the DSS reference location and (iii) the delay between B and the DSS reference location. The Ka-up/Ka-down band portable ZDD was designed and built to determine the delay of the test translator path A to B. The portable ZDD includes bandpass filters and isolators to suppress potential higher order harmonic distortion errors. Programmable 1-dB and 10-dB step attenuators are included in the downlink path to adjust the power level. The portable ZDD delay is precisely calibrated in the laboratory. A calibration method to determine the test translator delay can be described in five steps: (1) Perform normal station delay calibration with the test translator; (2) substitute the portable ZDD and its cables for the test translator path between A to B; (3) insert the portable ZDD for station delay calibration; (4) remove the pre-determined portable ZDD delay from the Step 3 measurement; and (5) calculate the test translator delay by using the normal station delay measured in Step 1 and subtracting the computed value at Step 4.

VI. Advanced Ranging Processor

A. Signal Acquisition and Range Extraction

There are three signals to be acquired and tracked by the software. The carrier is first detected using fast Fourier transform (FFT) acquisition. Once the carrier is acquired and in phase-lock, using a phase locked loop (PLL), the carrier model is scaled to the code clock and PN code frequencies to assist acquisition and tracking of these signals.

The two code clock tones (code clock plus and code clock minus) are processed without further acquisition by using the scaled carrier model. The software can be configured to track these tones with a PLL, or only use scaling of the carrier model, effectively forming an open-loop observation of these tones.

The PN code is acquired using parallel acquisition of the six shorter PN codes. During this open-loop phase of the PN code processing, the scaled carrier model is used to keep the integrations on-frequency. Once a high enough signal-to-noise ratio (SNR) is reached for each individual PN code, the Chinese Remainder Theorem is used to solve for the integer chip ambiguity of the full-length PN code, nominally 1009470 chips. At this stage, the full PN code model is used to correlate against the incoming signal, with a delay lock loop steering the early, prompt, and late correlators.

The code clock range observable is formed by differencing the upper and lower code clock phase observables. This range measurement is ambiguous to one cycle, and to form the full range observable, the integer portion of the PN code observable is used to remove the one-cycle code clock ambiguity.

The Advanced Ranging Processor (ARP) software computes observed range by evaluating the model used for integration at the center of the integration interval and adding in the residual.

B. Test and Validation

Validation of the ARP software is done in multiple stages. A signal simulator is first used to generate T2B/T4B signals modulated on a carrier with known range, velocity, and acceleration. The simulator generates a baseband complex voltage file, similar to the OLR. This voltage file is then processed using ARP, and the ARP-extracted range is compared against truth.

The second validation stage used real signals transponded by Juno (2017-123, 2 Mchip/s DSN PN code), where two independent software processors were used to measure phase in cycles at the range code clock frequency. The ARP and Delta-DOR (Delta Differential One-Way Ranging) software processing results agreed very well in the range measurement. Figure 4 shows the processing difference for 2-sec averages (blue) of spacecraft range signal, and the mean and the standard deviation of them are $\mu = 0.00305$ m, $\sigma = 0.67995$ m. Figure 5 shows the processing difference for 2-sec averages (blue) of test translator range signal, and the mean and the standard deviation of them are $\mu = 0.0061$ m, $\sigma = 0.07243$ m.
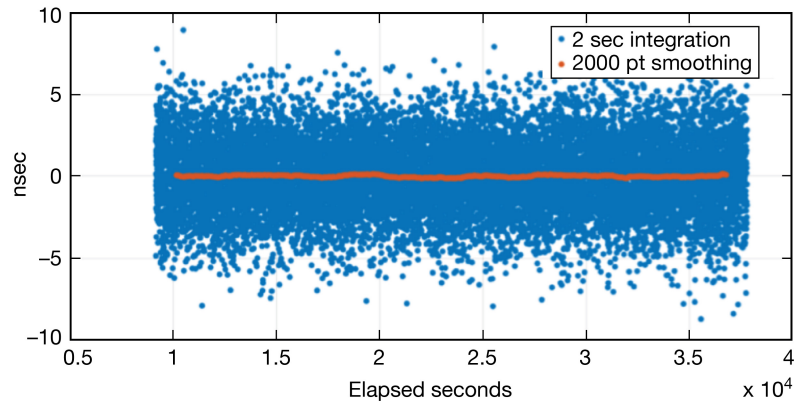
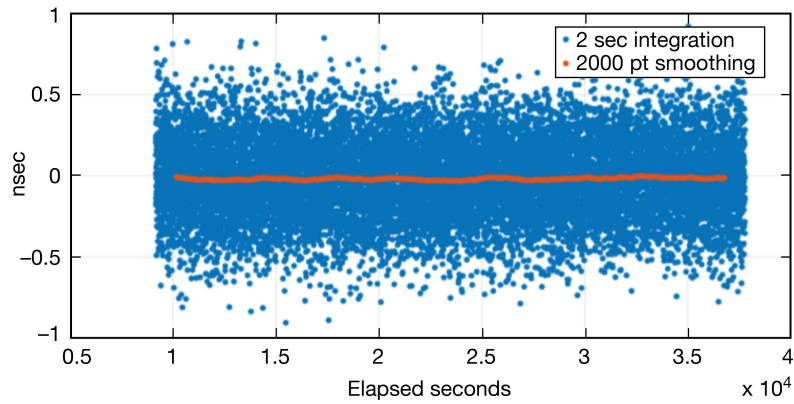**Figure 4. 2 Mchip/s, differences of phase for spacecraft.**

Figure 5. 2 Mchip/s, differences of phase for test translator.

A similar experiment was performed with a 24 Mchip/s PN code at DSS-25 for test translator range signal (2017-319), and again the code clock phase was compared against the two processors with excellent agreement. Figure 6 shows the processing difference for 1-sec averages (blue) of test translator range signal, and the mean and the standard deviation of them are $\mu = 0.000212$ m, $\sigma = 0.006125$ m.
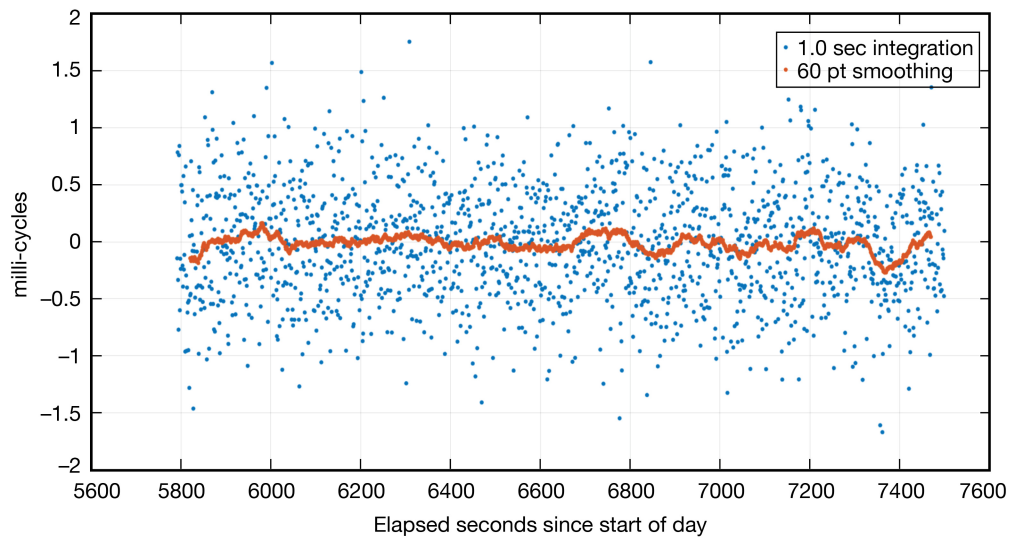

Figure 6. 24 Mchip/s, differences of phase for test translator.

The last validation performed was forming the full observed range of Juno (2017-123, 2 Mchip/s DSN PN code), which consists of forming a spacecraft range and test translator range, then subtracting these two ranges. The spacecraft and test translator range are formed using the upper-minus-lower code clock components and then adding in the integer part of the PN code range. This range is compared to DTT, which forms a real-time measurement of the spacecraft range, minus station delay, which was measured by DTT and 166570.65 range unit (RU). Figure 7 shows the processing difference of ARP and DTT for 200-sec averages. The average agreement between these two processors for the duration of the pass was $\mu = 0.00676$ m, $\sigma = 0.31$ m.
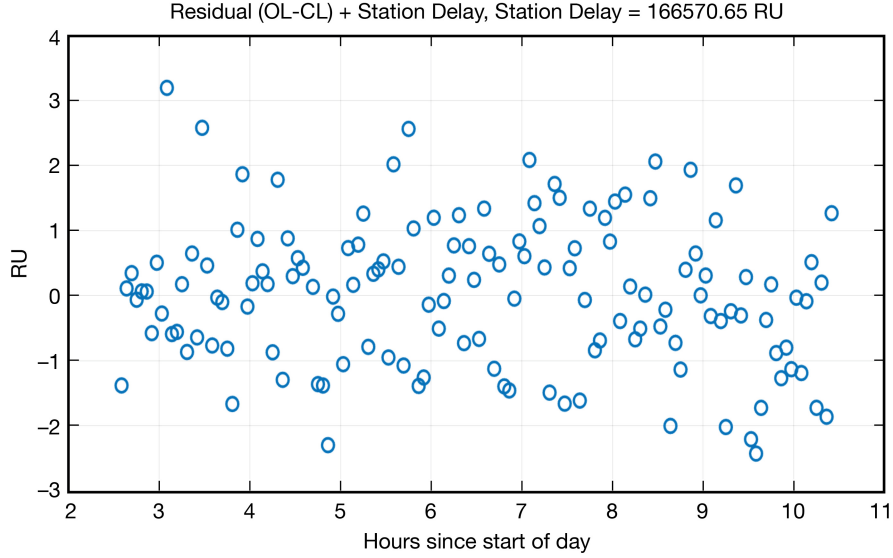

Figure 7. ARP-DTT residual, 1 RU ~0.94 ns for 2 Mchip/s range code.

VII. Plasma Noise Cancellation

The signals for all downlinks are recorded open loop. These include an X/X link, an X/Ka link, and a Ka/Ka link. Both the translated test signal and the received spacecraft signal are measured by ARP for each link. For the example of three links, there would be six time series of measured range code phase. These data are provided in the format of a tracking data message (TDM) [9]. It is left to the science data processing system to combine the time series to generate calibrated ranging observables. The formulation given in Equation 3 could be used to form the ranging observable for each individual link. Alternatively, it may be found that calibration is improved by taking the average of the station delays at the uplink and downlink times. Finally, a linear combination of the multi-link observables can be made to produce an observable that is free of charged particle effects.

The three received signals are affected by charged particle delays on the uplink, by charged particle delays on the downlink, and by the nondispersive range that is the object of the measurement. At microwave frequencies, charged particle delays are proportional to the inverse of the frequency squared. Since the spacecraft transponder turnaround ratios are not the same for the X/X and Ka/Ka links, these two links alone cannot remove the roundtrip charged particle delays. There are three linear equations in three unknowns to

solve for the nondispersive range ρ_{ND}, the uplink charged particle density TEC_{UL}, and the downlink charged particle density TEC_{DL}:

$$\rho_{XX} = \rho_{ND} + \frac{A * TEC_{UL}}{f_X^2} + \frac{A * TEC_{DL}}{\left(m_{XKa} f_X\right)^2} \tag{4}$$

$$\rho_{XKa} = \rho_{ND} + \frac{A * TEC_{UL}}{f_X^2} + \frac{A * TEC_{DL}}{\left(m_{XKa} f_X\right)^2} \tag{5}$$

$$\rho_{KaKa} = \rho_{ND} + \frac{A * TEC_{UL}}{f_{Ka}^2} + \frac{A * TEC_{DL}}{\left(m_{KaKa} f_{Ka}\right)^2} \tag{6}$$

where

ρ_{XX} = Observed range on X/X link

ρ_{XKa} = Observed range on X/Ka link

ρ_{KaKa} = Observed range on Ka/Ka link

m_{XX} = transponder turnaround ratio for X/X link (= 880/749 for BepiColombo)

m_{XKa} = transponder turnaround ratio for X/Ka link (= 3344/749 for BepiColombo)

m_{KaKa} = transponder turnaround ratio for Ka/Ka link (= 3360/3599 for BepiColombo)

A = units conversion constant, known

f_X = X-band uplink frequency, known ($\approx$ 7166935900 Hz for BepiColombo)

f_{Ka} = Ka-band uplink frequency, known ($\approx$ 34384220000 Hz for BepiColombo)

The solution for ρ_{ND} is:

$$\rho_{ND} = \frac{f_{Ka}^2}{f_{Ka}^2 - f_X^2} \rho_{KaKa} + \frac{m_{XX}^2 - m_{KaKa}^2}{m_{XKa}^2 - m_{XX}^2} \frac{f_X^2}{f_{Ka}^2 - f_X^2} \rho_{XKa} + \frac{m_{XX}^2}{m_{KaKa}^2} \frac{m_{KaKa}^2 - m_{XKa}^2}{m_{XKa}^2 - m_{XX}^2} \frac{f_X^2}{f_{Ka}^2 - f_X^2} \rho_{XX}. \tag{7}$$

Using the specific parameter values for BepiColombo, the equation for ρ_{ND} is approximately given by:

$$\rho_{ND} = 1.0454 * \rho_{KaKa} + 0.0285 * \rho_{XKa} - 0.0739 * \rho_{XX}. \tag{8}$$

The magnitudes of the coefficients imply that the performance of the linearly combined signal link is essentially the same as for the Ka/Ka link, but with charged particle effects removed. Errors in the other two links are reduced by the small coefficients and barely affect performance.

VIII. Summary

The precision radiometric tracking system at DSS-25 has been enhanced to include the capability for ranging with a Ka-band uplink. The CCSDS T2B and T4B PN codes as well as the DSN PN code are supported. The chip rate can be as high as 24 Mchip/sec at Ka-band. Open-loop techniques are used to record the ranging signal received from the spacecraft in addition to the station uplink fed back directly to the receiver through the test translator. The signal from the test translator provides a continuous measurement of station delay, allowing variations in the station instrumental path delay to be calibrated out during the pass.

Signal-processing software has been written to run on a server at Goldstone to extract ranging code phase from the open-loop recordings. This is done for both the spacecraft signal and the test translator signal. If there are multiple frequency links at X/X, X/Ka, and Ka/Ka, the range code phase measurements are made for each link. The range code phase measurements are provided to users in a TDM format [3]. The users can generate ranging observables for each frequency link from the data. The equations for generating observables are documented in this report. A linear combination of observables from the multiple links can be applied by the user to obtain a ranging observable that is free of charged particle effects. The open-loop technique was validated with a pass of ranging using the DSN PN code transmitted to Juno at X-band. The open-loop data agreed quite well with the DTT data.

For spacecraft that support multi-frequency links and support high range code chip rates, better ranging accuracy than what is available at X-band only can be obtained. The multiple frequency links eliminate errors due to charged particles. The higher chip rate reduces the effect of instrumental phase errors in the order of 1 degree that are always present, since the effective range code wavelength is small for high chip rates. Regeneration of the PN code in the spacecraft transponder, combined with the higher chip rate, reduces the error due to thermal noise. Ranging accuracy in the order of 10 cm is expected for spacecraft with advanced transponders. The first opportunity to demonstrate the full capability of the new ranging system will be the ESA spacecraft BepiColombo.

References

[1] L. Iess, S. Asmar, and P. Tortora, "MORE: An advanced tracking experiment for the exploration of Mercury with the mission BepiColombo," *Acta Astronautica,* vol. 65, no. 5-6, pp. 666–675, 2009.

[2] B. Bertotti, L. Iess, and P. Tortora, "A test of general relativity using radio links with the Cassini spacecraft," *Nature,* vol. 425, pp. 374–376, 2003.

[3] *Pseudo-Noise (PN) Ranging Systems,* Recommendation for Space Data System Standards, CCSDS 414.1-B-2, Blue Book, February 2014.

[4] J. B. Berner, S. H. Bryant, and P. W. Kinman, "Range measurement as practiced in the Deep Space Network," *Proceedings of the IEEE,* vol. 95, no. 11, pp. 2202–2214, 2007.

[5] J. S. Border, G. E. Lanyi, and D. K. Shin, "Radiometric Tracking for Deep Space Navigation," in *31th Annual AAS Guidance and Control Conference,* Breckenridge, Colorado, 2008.

[6] P. Kuchynka, W. M. Folkner, and A. S. Konopliv, "Station-Specific Errors in Mars Ranging Measurements," *IPN Progress Report,* Vols. 42-190, pp. 1–11, August 2012.

[7] J. S. Border and M. Paik, "Station Delay Calibration for Ranging Measurements," *IPN Progress Report,* Vols. 42-177, pp. 1–14, May 2009.

[8] D. D. Morabito, R. Mendoza, D. Highsmith, J. S. Border, and S. Shambayati, "Analysis of Ka-Band Radiometric Data Acquired during Cruise of the Mars Reconnaissance Orbiter," *Proceedings of the 12th Ka and Broadband Communications Conference,* pp. 259–266, 27–29 September 2006.

[9] *DSN Document 820-013, 0212-Tracking-TDM, DSN Tracking Data Message (TDM) Interface, Rev D,* JPL D-16765, October 2015.